Environmental Science & Technology

Article

pubs.acs.org/est

Interactions of Microorganisms with Polymer Nanocomposite Surfaces Containing Oxidized Carbon Nanotubes

David G. Goodwin, Jr.,[†] K. M. Marsh,[†] I. B. Sosa,[‡] J. B. Payne,[§] J. M. Gorham,[∥] E. J. Bouwer,[§] and D. H. Fairbrother*,[†]

[†]Department of Chemistry, Johns Hopkins University, Baltimore, Maryland 21218, United States

[‡]Centro de Química, Instituto Venezolano de Investigaciones Cientificas (IVIC), Altos de Pipe, Caracas 1020-A, Miranda, Venezuela

[§]Department of Geography and Environmental Engineering, Johns Hopkins University, Baltimore, Maryland 21218, United States

[∥]Materials Measurement Science Division, NIST, Gaithersburg, Maryland 20899, United States

Supporting Information

ABSTRACT: In many environmental scenarios, the fate and impact of polymer nanocomposites (PNCs) that contain carbon nanotubes (CNT/PNCs) will be influenced by their interactions with microorganisms, with implications for antimicrobial properties and the long-term persistence of PNCs. Using oxidized single-wall (O-SWCNTs) and multi-wall CNTs (O-MWCNTs), we explored the influence that CNT loading (mass fraction ≤0.1%−10%) and type have on the initial interactions of *Pseudomonas aeruginosa* with O-CNT/poly(vinyl alcohol) (PVOH) nanocomposites containing well-dispersed O-CNTs. LIVE/DEAD staining revealed that, despite oxidation, the inclusion of O-SWCNTs or O-MWCNTs caused PNC surfaces to exhibit antimicrobial properties. The fraction of living cells deposited on both O-SWCNT and O-MWCNT/PNC surfaces decreased exponentially with increasing CNT loading, with O-SWCNTs being approximately three times more cytotoxic on a % w/w basis. Although not every contact event between attached microorganisms and CNTs led to cell death, the cytotoxicity of the CNT/PNC surfaces scaled with the total contact area that existed between the microorganisms and CNTs. However, because the antimicrobial properties of CNT/PNC surfaces require direct CNT-microbe contact, dead cells were able to shield living cells from the cytotoxic effects of CNTs, allowing biofilm formation to occur on CNT/PNCs exposed to *Pseudomonas aeruginosa* for longer time periods.

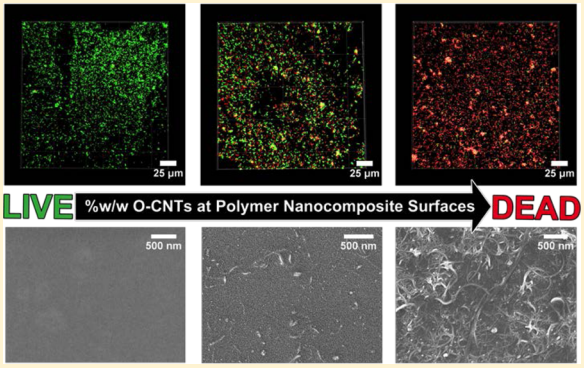

INTRODUCTION

One of the most important projected commercial applications of engineered nanomaterials (ENMs) such as carbon nanotubes (CNTs), nanosilver, and nanoscale metal oxides involves their use as fillers in polymer matrices at low concentrations, typically at a mass fraction of less than 5% w/w, to produce polymer nanocomposites.[1−6] The advantage of incorporating ENMs into polymers derives from their ability to greatly expand the material's value and utility by enhancing numerous polymer properties.[6−8] Carbon nanotubes are becoming one of the most widely studied fillers in view of their large aspect ratio and excellent thermal, chemical, and mechanical properties. This collection of desirable attributes makes them ideal candidates to improve tensile strength, elastic modulus, thermal conductivity, and current carrying capacities of polymers.[9−22] For example, multi-wall CNT (MWCNT) - polystyrene nanocomposites containing only 1% w/w MWCNTs exhibit a 36−42% increase in elastic modulus and a 25% increase in break stress relative to pure polystyrene.[16] Consequently, CNT-containing nanocomposites are already present in a diverse array of products that include bicycles, tennis racquets, sail boats, antistatic parts for fuel filter lines, and packaging materials used in the electronics industries.[23−27]

As the use of CNTs embedded in polymer matrices increases, it is inevitable that a significant fraction of commercially produced CNTs will first enter the environment embedded in plastic materials.[28−30] Thus, it is important to understand the behavior of CNT/PNCs in the environment.[28,31−33] One of the situations that will determine the fate of CNT/PNCs occurs at the end of their life cycle where disposal follows consumer use. Under these conditions, the impact and persistence of a CNT/PNC will depend on its interactions with microbial populations present in landfills. Other CNT/PNCs will be improperly disposed of on land (i.e., litter) and in surface waters where they can also encounter and interact with a wide variety of microorganisms.

Received: January 6, 2015
Revised: March 21, 2015
Accepted: March 26, 2015
Published: March 26, 2015

DOI: 10.1021/acs.est.5b00084
Environ. Sci. Technol. 2015, 49, 5484−5492

The first step in the interaction of microbes with solid substrates is the attachment of planktonic cells to the surface followed by growth and colonization. If the microorganisms survive upon surface attachment, they colonize through proliferation and produce extracellular polymeric substances (EPS) to form biofilms.[34,35] In contrast, if the surface exhibits antimicrobial properties, cell proliferation can be retarded or even inhibited.[36,37] If biofilm formation occurs, the metabolic activity of the attached microorganisms can initiate biodegradation through the release of extracellular enzymes.[38−41] Thus, the initial interactions of microorganisms with CNT/PNCs will play an important role in determining the nanomaterial's long-term fate and persistence.

In the majority of studies involving CNTs and microorganisms, antimicrobial properties have been observed regardless of whether the CNTs were dispersed or aggregated in the aqueous phase or collected on a membrane or surface.[28,42−48] For example, surfaces coated with pristine SWCNTs markedly reduced the amount of *Escherichia coli* that could form a biofilm due to the antimicrobial nature of the surface.[42] Three of the main mechanistic hypotheses for CNT cytotoxicity include puncturing of the cell membrane, membrane disruption, and oxidative stress.[43,44,49−53]A smaller number of studies, however, have claimed that CNTs exhibit weak or no observable cytotoxic response toward microbes.[54−56] Thus, Pantanella et al. found that SWCNT-coated surfaces do not affect adhesion or biofilm formation and attributed this to a lack of antimicrobial properties for selected bacterial species.[56] Therefore, the cytotoxicity of CNTs remains controversial.[57,58]

In the case of CNT/PNCs, a few studies have evaluated the influence of pristine CNTs exposed at the surface of PNCs on cell death. For example, polyvinyl-N-carbazole (PVK) nanocomposites containing only 3% w/w SWCNTs caused significant cell death (>80%) of *Escherichia coli* and *Bacillus subtilis* relative to pure PVK. MWCNTs embedded in the same polymer also led to significant cytotoxicity.[47,59] Similarly, Schiffman et al. found that the inclusion of pristine SWNTs in electrospun polysulfone fibers caused an increase in cell death as the SWNT concentration increased from 0−1% w/w.[60] Consequently, it has been suggested that CNT-modified materials can serve as antimicrobial coatings to resist biofouling or biofilm formation in applications ranging from medical devices to membranes, piping, and boat hulls.[27,49,61,62]

In nanocomposite products, cycles of weathering and biodegradation can eventually cause CNTs to reach the surface and to potentially even accumulate, regardless of whether or not the CNTs are initially exposed at the PNC surface or buried under a thin polymer layer or surface coating.[30,63−65] Under these conditions, the interactions of microorganisms with CNT/PNC surfaces will be important during the life cycle of the material. To date, studies on the interactions of microbes with CNTs embedded in polymeric matrices or in membranes have focused on pristine CNTs. In contrast, we have focused on the antimicrobial properties of oxidized single- and multi-wall CNTs embedded in CNT/PNCs. This decision was motivated by the likelihood that many pristine CNTs initially introduced into PNCs will have their surfaces oxidized by weathering in landfills and other environments prior to their interactions with microorganisms.[66,67]

To explore the initial interactions of microorganisms with CNT/PNCs, oxidized CNTs (O-CNTs) were well-dispersed in poly(vinyl alcohol) (PVOH), which was chosen as the polymer matrix due to its lack of antimicrobial properties, allowing the effect of CNT inclusion to be clearly delineated.[68,69] CNT/PVOH nanocomposites were exposed to the Gram-negative microorganism *Pseudomonas aeruginosa*, a model aquatic and soil bacterium that can readily proliferate to form biofilms. Indeed, *Pseudomonas* species are ubiquitous in the environment where they are likely to encounter plastic waste and are frequently responsible for biodegradation of organic matter and organic contaminants.[70] The interaction of *P. aeruginosa* with CNT/PNCs containing O-CNTs of different type (O-MWCNT vs O-SWCNT) and CNT loading (0−10% w/w) was assessed using SYTO 9 and propidium iodide fluorescent stains to differentiate living and dead bacteria, as measured by the integrity of the cell membrane. This study was motivated by the desire to provide insights into the initial interaction of microorganisms with CNT/PNC surfaces having different CNT concentrations, representative of nanocomposite surfaces that may be present following weathering and/or other environmental degradation processes.

EXPERIMENTAL SECTION

O-CNT/PVOH Nanocomposite Preparation. A 2 mg/mL stock solution of poly(vinyl alcohol) (PVOH) was prepared by dissolving PVOH (Sigma-Aldrich, M_w = 31,000−50,000, 98%−99% hydrolyzed) into deionized water while stirring at 105 °C for 4 h. The solution was filter-sterilized using a 0.2 μm acetate filter. A 0.05 mg/mL O-MWCNT stock suspension (NanoLab Inc., PD15L5-20-COOH, Lot. # 06-6-10, outer diameter 15 ± 5 nm, length 5−20 μm from the manufacturer) was prepared by sonicating 10 mg of O-MWCNTs into 200 mL of deionized water for ∼20 h using a Branson 1510 ultrasonic bath operating at 70 W. The stock suspension was then centrifuged (5 min, 3000 rpm, Powerspin LX, Unico) to remove glass etched during sonication and some larger CNT bundles for a final concentration of slightly less than or equal to 0.05 mg/mL; the same stock solution was used throughout this study. The same procedure was followed for O-SWCNTs (Carbon Solutions, P3-SWNT, Lot # 03-A014, outer diameter of individual or bundles 1−5 nm, length 1 ± 0.5 μm).

Immediately prior to spray-coating, the stock PVOH solution and stock O-CNT suspensions (O-MWCNTs and O-SWCNTs) were combined aseptically in different volume ratios to prepare casting solutions containing 0, 0.1, 1, 5, and 10% w/w O-CNT/PVOH. Each casting solution was shaken vigorously, sonicated for 5 min, and added to a spray bottle capable of nebulizing the solution. Autoclaved glass slides (1 × 25 × 75 mm) were placed onto a hot plate at 150 °C and sprayed from a consistent distance (approximately 25 cm) in 10 s intervals to flash dry the casting solution upon contact (Figure S1). This helped to minimize CNT aggregation during the drying process. Casting solutions were sprayed 30 times (1.07 mL/spray ± 0.05 mL/spray) to fully cover the glass slides with CNT/PNC. The uniformity and average thickness of the coating was determined by measuring the decrease in the Si(2p) signal from the underlying glass substrate using X-ray photoelectron spectroscopy (XPS) on different, randomly selected regions of a PVOH and 10% w/w O-MWCNT/PVOH nanocomposite.[71,72] This analysis revealed that regardless of CNT/PNC type, the average thickness of the overlayer was ≈8 nm; further information on how film thicknesses were determined can be found in the SI. All spray-coating was carried out inside a sterile biosafety cabinet (Labconco Purifier Class II Biosafety Cabinet). To verify

DOI: 10.1021/acs.est.5b00084
Environ. Sci. Technol. 2015, 49, 5484−5492

consistency in the preparation and properties of the nanocomposites, replicate samples (at least in duplicate) of each nanocomposite type (0−10% w/w) were prepared separately and studied in terms of their initial interactions with microorganisms.

CNT/PVOH Nanocomposite Characterization. *Scanning Electron Microscopy (SEM) and X-ray Photoelectron Spectroscopy (XPS).* Procedures for XPS and SEM imaging of PVOH and O-CNT/PVOH samples are outlined in the SI. Replicate SEM images of different nanocomposite areas and separately sprayed slides are shown for each nanocomposite type in Figure S2. Spectra of O-SWCNT/PVOH nanocomposites are shown in Figure S3.

Dissolution Controls. To ensure PVOH dissolution did not have an effect on this study, high M_w PVOH (M_w = 31,000−50,000) was used since it is less susceptible to dissolution compared to lower M_w analogues. Nevertheless, qualitative SEM control experiments were run to verify that CNT/PNCs did not change in surface composition, specifically in terms of the relative concentration of CNTs, over the short time course of our immersion experiments (1−6 h, Figures S4 and S5). Further information can be found in the SI.

The upper limits of metal ion (from residual metal catalyst impurities in CNTs) and CNT release that could occur during 1 h of nanocomposite immersion were assessed in separate experiments using ICP-MS. In both cases, the experiments involved exposing the highest loading of O-SWCNTs in PVOH (10% w/w) to sterile milli-Q water (BMM) for 1 h. To determine the concentration of metal ions released, the supernatant that was generated after 1 h was filtered through a 0.02 μm glass fiber membrane to remove all particulate matter, and the metal ion concentration in the filtrate was measured with ICP-MS. This analysis revealed that the yttrium ion concentration in the supernatant was at or below the detection limit of the ICP-MS (<1 ppt). In contrast, the concentration of released CNTs was determined by analyzing the supernatant (no filtration) for the presence of yttrium nanoparticles as a proxy for CNTs, as described in our previous publication, using ICP-MS in single particle mode (sp-ICP-MS).[73] Using this method we determined that the upper limit of the released CNT concentration from the nanocomposites was approximately 90 ppb after 1 h immersion time in sterile milli-Q water. Further information can be found in the SI.

Microbial Growth and O-CNT/PVOH Nanocomposite Inoculation (1 and 6 h). To assess the effect of CNT loading on the antimicrobial properties of O-CNT/PVOH nanocomposites, the initial cytotoxicity of *P. aeruginosa* (ATC 27853) on CNT/PNC surfaces was determined. Each O-CNT/PVOH slide was submerged in a Petri dish containing 15 mL of exponential phase *P. aeruginosa* in BMM under ambient conditions. The nanocomposite slides were then removed from the inoculum after 1 or 6 h, washed with depleted media, and immediately transferred into fresh sterile Petri dishes for subsequent LIVE/DEAD staining. Each CNT/PNC sample of a particular CNT loading was exposed to three separately grown *P. aeruginosa* cultures to ensure consistency in the number of attached cells between cultures. Examples of the reproducibility of the data acquired from these replicates are shown for PVOH, 10% w/w O-MWCNT/PVOH, and 10% w/w O-SWCNT/PVOH in Figure S6. Similarly, we verified that for each nanocomposite type (0−10% w/w), the number of attached cells was statistically the same for samples that were spray-coated on different occasions. Media composition, growth conditions, and 6 h LIVE/DEAD images are described in the SI (Figures S7−S9).

To assess the possibility that released CNTs could affect the microorganisms in solution, two separate growth curves were conducted in the presence of 90 ppb O-MWCNTs and 90 ppb O-SWCNTs. These CNT concentrations were selected because they represent the upper limit of released CNTs observed during the course of our release control experiments using sp-ICP-MS. Results from these growth curves revealed that there was no effect at these low (ppb) CNT concentrations relative to a growth curve without CNTs. Indeed, previous studies have shown that CNT concentrations in the ppm range are typically needed to inhibit cell growth.[48] Results of this analysis can be found in the Supporting Information (Figure S8 and related text).

LIVE/DEAD Staining. A FilmTracer LIVE/DEAD Biofilm Viability Kit (Molecular Probes, Invitrogen) containing SYTO 9 and propidium iodide (PI) stains was used.[74] At least 15 images per CNT loading prepared at different times (at least two different occasions) and exposed to three different cultures were analyzed to determine the average percentage and standard deviation of living *P. aeruginosa* cells on a given CNT/PNC slide. Positive and negative controls for cytotoxicity were run: these included staining microbes attached to PVOH (0% w/w O-CNTs) and microbes purposely lysed with ethanol on PVOH (Figure S10), respectively. Further details, as well as a significant number of experimental controls, can be found in the SI (Figures S11−S15). A FilmTracer SYPRO Ruby Red Biofilm Viability Kit (Invitrogen, Life Technologies) was used to stain the EPS on PVOH, 10% w/w O-MWCNT/PVOH, and 10% w/w O-SWCNT/PVOH samples after 1 h of microbial exposure (Figure S16). Background fluorescent controls were run for this stain as well (Figure S17).[75]

Confocal Laser Scanning Microscopy (CLSM). Microbes on CNT/PNC surfaces stained with SYTO 9 and PI were imaged using a Zeiss LSM 510 Multiphoton Confocor 3 CLSM with a 40× water immersion objective (N.A. 1.2) to generate dual channel 3D images for each sample. Further information can be found in the SI.

RESULTS AND DISCUSSION

CNT/PNC Characterization. While the SEM images of pure PVOH exhibited surfaces devoid of any cylindrical, CNT-like structures (Figure 1), the presence of CNTs at the surface of O-CNT/PVOH nanocomposites became increasingly apparent as a function of increasing CNT loading. SEM images also show O-SWCNTs and O-MWCNTs randomly distributed across the surface with minimal signs of aggregation across the range of CNT loadings studied (0−10% w/w). The uniformity of the surface is demonstrated by the consistency of SEM images acquired in different, randomly selected regions (Figure S2a-i).

To complement SEM data, XPS analysis was performed for PVOH nanocomposites with varied O-MWCNT loadings (≥5% w/w), with the goal of evaluating the CNT concentration at the O-CNT/PVOH surfaces (Figure 2). For O-MWCNT/PVOH nanocomposites, the C(1s) spectral envelope could be well fit by contributions from the PVOH and the CNT components, along with a small (≤7.5%) contribution from amorphous carbon contamination. The ability to determine the O-MWCNT surface concentration from the C(1s) fitting protocol can be attributed to the differential charging behavior of PVOH and the O-MWCNTs,

DOI: 10.1021/acs.est.5b00084
Environ. Sci. Technol. 2015, 49, 5484−5492

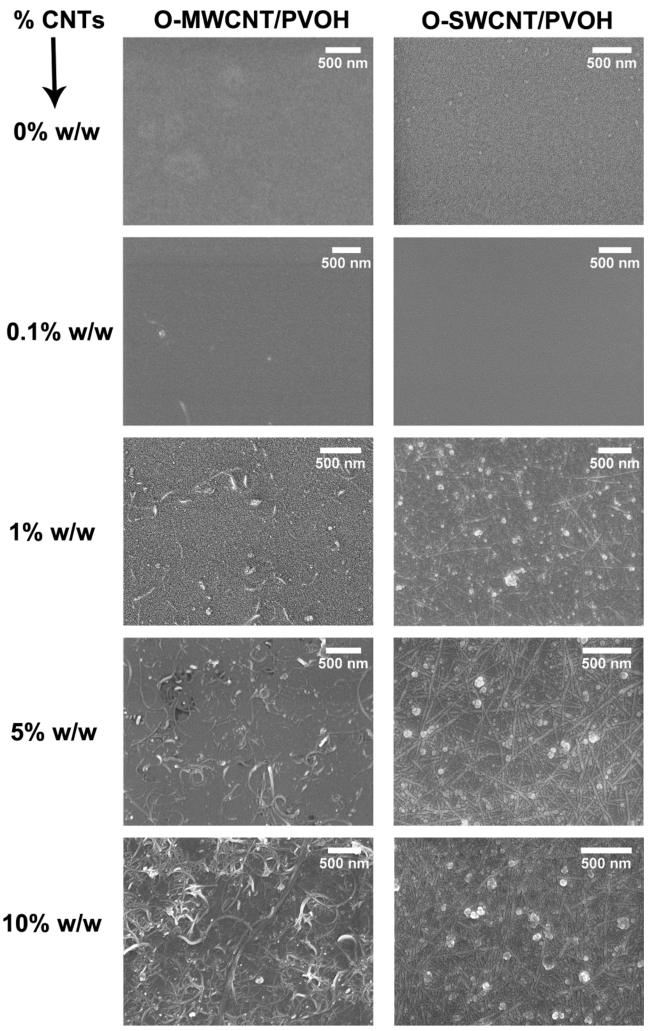

Figure 1. SEM images of well-dispersed, spray-dried O-MWCNT/PVOH and O-SWCNT/PVOH nanocomposites as a fraction of CNT loading ranging from 0 to 10% w/w.

which effectively separates their spectral envelopes.[32,76] In contrast to the behavior of O-MWCNT/PVOH nanocomposites, O-SWCNT/PVOH nanocomposites did not differentially charge to an extent that permitted spectral deconvolution of the individual components (Figure S3).

XPS analysis of the C(1s) region indicates that the O-MWCNT concentration at the surface in the % w/w region under investigation (<10% w/w) should be directly proportional to the composition of the casting solution (R^2 = 0.92) (Figure 2). We attribute this proportionality in large part to a consequence of the flash drying method used to prepare the CNT/PNCs, which greatly restricts CNT aggregation and essentially "locks" their structure and composition within the polymer into a close representation of the O-CNT/PVOH distribution in the casting solution.

Antimicrobial Properties of CNT/PNCs. Figures 3 and 4 show representative results of LIVE/DEAD staining used in conjunction with CLSM to assess the cytotoxicity of *P. aeruginosa* attached to O-MWCNT and O-SWCNT/PVOH surfaces after 1 h of inoculation. This time period was selected because it was sufficient for >1500 microbes to attach directly onto the CNT/PNC surfaces and therefore provide a statistically significant measure of the surface's initial antimicrobial properties. Cells that were considered attached were those that remained on the nanocomposite surfaces during the staining procedure. Living and dead cells were counted using image analysis software, and results are shown in Figure 5. For PVOH, the CLSM image is dominated by green fluorescent cells, indicating that PVOH is benign to *P. aeruginosa*. In contrast, the antimicrobial properties of the CNT/PNC surfaces increased systematically with both O-MWCNT and O-SWCNT loading as evidenced by the increasing number of red fluorescent cells (Figures 3 and 4). Consequently, the antimicrobial properties exhibited by the O-CNT/PVOH nanocomposite surfaces are due to the inclusion of O-CNTs (Figures 3 and 4).

At the highest O-MWCNT and O-SWCNT loadings of 10% w/w, virtually all (>90%) of the *P. aeruginosa* fluoresced red, indicating that the majority of cells had died. However, longer term (6 h) experiments conducted on 10% w/w O-MWCNTs (Figure 3) showed evidence of healthy (green) biofilm formation for microorganisms located on top of dead cells (red). Similarly, careful analysis of the CLSM images acquired after 1 h of contact time between the *P. aeruginosa* and the CNT/PNC surfaces revealed that some of the living microorganisms are actually deposited on top of dead microorganisms. CLSM analysis of these "live on top of dead" structures exhibited heights in the range of ∼4−7 μm. In contrast, individual microorganisms attached to the surfaces had apparent heights of ∼4−5 μm. It should be noted that in CLSM, the height of the microbes appears stretched and taller than their actual height (0.5−1 μm) due to the limited vertical resolution of the CLSM (>1 μm) compounded by fluorescence scattering between optical slices (Figures S18 and S19).[70] Thus, "live on top of dead" structures were consistent with about two microbial layers, with living cells located on top of dead cells, the latter in direct contact with the CNT/PNC surfaces. Examples of this phenomenon are circled in white for 1% w/w O-CNT/PVOH samples (Figures S18 and S19). The nature of these structures supports the idea that CNT contact is necessary to cause cell death.

Additional insights into the antimicrobial properties of CNTs observed during the initial stages of microbial attachment can be attained by considering the distribution and concentration of CNTs at the interface in relationship to the two-dimensional footprint of an attached *P. aeruginosa* microorganism, which is rod-shaped and approximately 1 μm in length by >0.5 μm wide, as revealed by SEM (Figure S20).[70] By superimposing this two-dimensional microbe footprint onto an SEM image of a PNC surface, we can gauge the degree of direct interaction/contact between attached *P. aeruginosa* microorganisms and CNTs at a particular CNT loading (Figures S18 and S19). As shown in Figure S19, this analysis reveals that the 1% w/w O-SWCNT/PVOH nanocomposite surface consists of a relatively dense O-SWCNT mesh, which is a reflection of the extremely high aspect ratio of CNTs (microsized lengths and nanometer-scaled widths). Consequently, most microorganisms that attach to the CNT/PNC surface must make contact with multiple CNTs (>5 CNTs). However, the corresponding CLSM image for 1% w/w O-SWCNTs shown in Figure 4 reveals that more than 20% of the attached microorganisms are still alive despite many appearing to be in direct contact with the underlying surface. Moreover, the distribution of living and dead microorganisms on the surface is entirely random with no evidence of any patchiness that would indicate a lack of CNT dispersion in localized areas. Thus, our experimental observations indicate that a single contact event or interaction between a CNT and

DOI: 10.1021/acs.est.5b00084
Environ. Sci. Technol. 2015, 49, 5484−5492

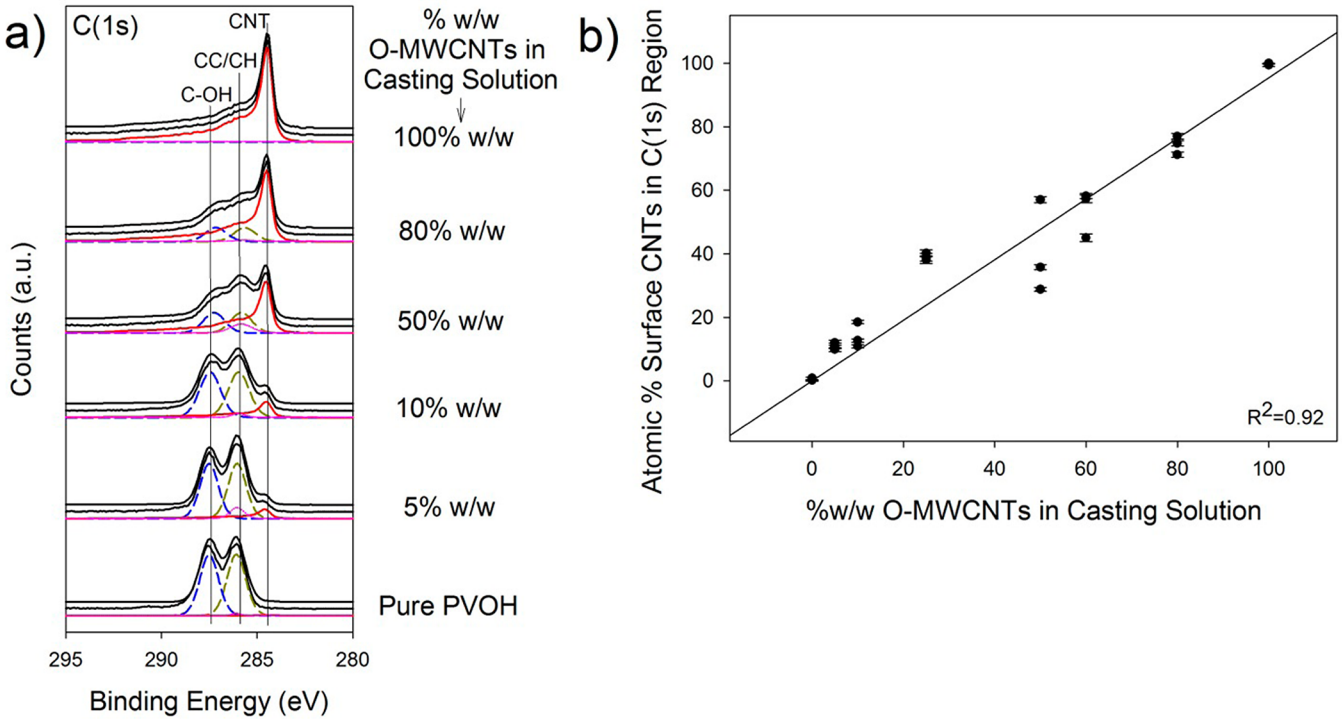

Figure 2. X-ray photoelectron spectroscopy (XPS) characterization of O-CNT/PVOH nanocomposites. a) C(1s) region of O-MWCNT/PVOH nanocomposites with increasing O-MWCNT loading. The fitted PVOH components (dashed lines) and the O-MWCNT component (solid line) are shown within the carbon envelope. b) % w/w O-MWCNTs in casting solution vs atomic % surface CNTs determined using XPS fitting of the C(1s) envelope. Error bars are reflective of the error in the fitting protocol for a given sample.

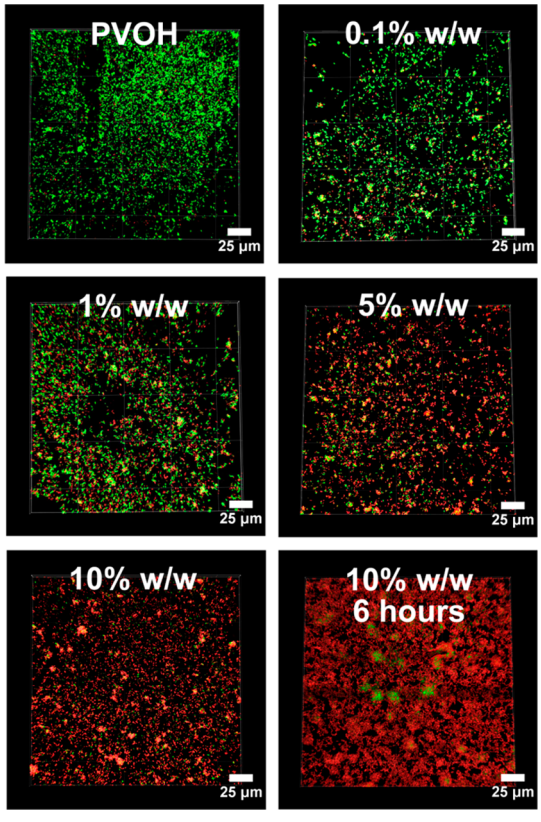

Figure 3. CLSM images of LIVE/DEAD stained *P. aeruginosa* grown statically for 1 h on O-MWCNT/PVOH slides with increasing O-MWCNT loading from 0−10% w/w and at 6 h on a 10% w/w nanocomposite.

an attached microorganism does not guarantee that the microorganism will die; otherwise, all of the attached *P. aeruginosa* on the 1% w/w O-SWCNT/PVOH nanocomposites surface would be dead, which is not the case.

We note that it is possible that not every CNT contact event with an adsorbed microorganism is disposed to cause membrane disruption. This would be the case, for example, if a specific interaction were required, such as the puncturing of the membrane by the exposed ends of a CNT. The amount of EPS excretion, a common defense used in biofilms to protect cells from environmental stressors,[42] was tested as it could serve to diminish the antimicrobial nature of the CNT/PNCs by effectively shielding attached bacteria from the CNTs. The level of EPS was shown to be minimal on the CNT/PNC surfaces after 1 h using a biofilm matrix stain (SYPRO Ruby Biofilm Matrix Stain), indicating that EPS excretion is not an important factor in the present study (Figure S16). Regardless of the detailed explanation of this phenomenon, once the O-SWCNT loading was increased to 10% w/w, almost all *P. aeruginosa* (97%) attached to the PNC surface experienced >5 CNT contact events. Under these circumstances, the number of CNT contact events and greater contact area between adsorbed microorganisms and surface-bound CNTs was apparently sufficient to cause almost all of the attached microorganisms to die (Figures 3 and 5). An analogous argument can be made for O-MWCNTs on the basis of the data shown in Figures 4 and 5. The present study is uniquely well-positioned to assess the role that contact area plays in determining the antimicrobial properties of CNTs because the distribution and concentration of CNTs at the surface has been well-defined through the use of SEM and XPS across a range of CNT loadings.

Our experimental data also clearly demonstrates that the antimicrobial properties of CNTs are not eliminated when they

DOI: 10.1021/acs.est.5b00084
Environ. Sci. Technol. 2015, 49, 5484−5492

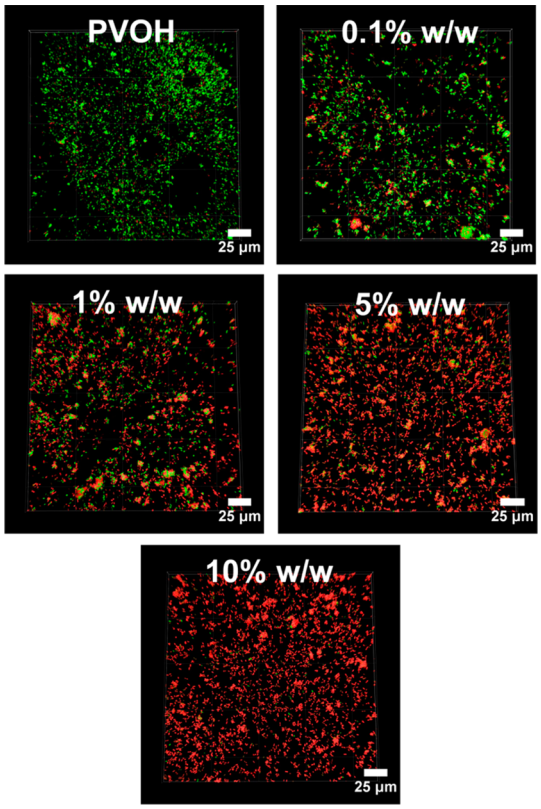

Figure 4. CLSM images of LIVE/DEAD stained *P. aeruginosa* grown statically for 1 h on O-SWCNT/PVOH slides with increasing O-SWCNT loading from 0 to 10% w/w.

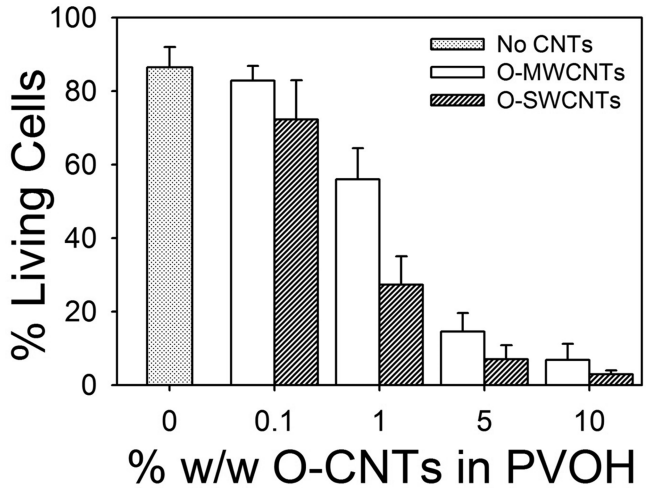

Figure 5. Live and dead cell counting of *P. aeruginosa* confocal images using image analysis software. The average percentage ± one standard deviation of attached living cells from ≥15 images of each O-MWCNT and O-SWCNT/PVOH nanocomposite loading (0−10% w/w) is shown.

are oxidized, regardless of type (SWCNT or MWCNT) or manufacturer (Carbon Solutions and NanoLab Inc., respectively). Figure S21 demonstrates that as a function of increasing CNT loading, the fraction of living cells deposited on both O-SWCNT and O-MWCNT/PVOH surfaces can be reasonably well fit with a first order exponential decay profile. On the basis of this analysis, the O-SWCNTs are approximately three times more cytotoxic than O-MWCNTs on a % w/w basis. We ascribe this enhancement of O-SWCNT/PVOH antimicrobial properties in part to a number density effect, since at the same CNT loading there is a greater number of O-SWCNTs than O-MWCNTs at the PNC surface. As a result, the number of contact events and total contact area between attached microbes and CNTs will always be greater for O-SWCNTs as compared to O-MWCNTs (Figure S22). Regardless, the antimicrobial properties of O-SWCNTs and O-MWCNTs do not differ markedly from one another as a function of CNT loading. We ascribe this similarity to be a consequence, at least in part, of the high oxygen levels on the CNTs used (8.6% O for O-MWCNTs, 9.2% O for O-SWCNTs as measured by XPS). This level of surface oxidation is expected to significantly disrupt the graphenic sidewall structure and cause the surfaces of O-SWNCNTs and O-MWCNTs to appear somewhat structurally and chemically similar, containing graphenic sidewalls, interspersed with defect regions (and ends) where oxygen-functional groups are localized.

Results from the present investigation can be compared with other related studies. For example, Schiffman et al. evaluated the cytotoxicity of pristine SWCNTs toward *E. coli*, another Gram-negative bacterium, as a function of SWCNT loading in electrospun polymer mats. As the loading of pristine SWCNTs increased from 0.1 to 1% w/w, cell death increased from 18% to 76%, respectively.[60] In the present study, the cytotoxicity we observed for *P. aeruginosa* increased from 27% to 73% cell death as the O-SWCNT loading increased from 0.1% to 1%, respectively. In another study, Rodrigues et al. saw 90% cell death of *E. coli* on MWCNT/poly(*N*-vinylcarbazole) nanocomposites with 6% w/w MWCNT, while in our studies on O-CNT/PVOH nanocomposites, we observed 86% cell death of *P. aeruginosa* for 5% w/w O-MWCNT.[59] Although the microorganisms and type of CNTs differed among these CNT/PNC studies, the similarities in the results are striking and suggest that the antimicrobial properties of CNT/PNCs toward Gram-negative bacteria may be broadly similar across a range of CNT types. Interestingly, in studies where pristine SWCNTs and MWCNTs were simply deposited onto surfaces, only 85% and 30% cell death occurred for *E. coli*, respectively.[43,44,77] Similar or even greater levels of cytotoxicity were observed in the present study for surfaces that contained ≤10% w/w CNTs. This suggests that the CNT dispersion state may also be important in determining antimicrobial properties.[43,44,47,59,77]

Although our experimental data does not provide a means to definitively prove which mechanism(s) are responsible for the cytotoxicity of oxidized CNTs, a mechanism that we can rule out in this study is one being caused by the release of metal ions from metal nanoparticles that are often present in CNTs (Figure S23). This was evaluated explicitly in the present study by using ICP-MS to measure the yttrium ion concentration released from O-SWCNT/PVOH nanocomposites (~0.2 ppt) after an hour of immersion in sterilized milli-Q water. Results showed that the metal ion concentration was at or below the detection limit of the ICP-MS (~0.1−1 ppt) (Figure S23), much lower than the typical concentrations within the parts per billion to parts per million range that can lead to an inhibitory effect on microbial growth.[78,79] Moreover, a cytotoxicity mechanism governed by the release of metal ions would be unlikely to require direct contact to exist between CNTs and the microorganisms. Cell death simply caused by an increase in hydrophobicity from an increase in CNT content was also ruled out by showing that a hydrophobic surface (poly-ε-

DOI: 10.1021/acs.est.5b00084
Environ. Sci. Technol. 2015, 49, 5484−5492

caprolactone) does not exhibit antimicrobial properties toward *P. aeruginosa* after 1 h of bacterial deposition (Figure S24). We note that most of the commonly proposed mechanisms that are used to explain CNT cytotoxicity could reasonably be expected to scale with the total contact area between attached microorganisms and polymer-surface bound CNTs. For example, the probability that the end of a CNT would align correctly so as to puncture the cell membrane of an attached microorganism should increase with the CNT-microorganism contact area.[43,44,49] A cytotoxicity mechanism that scaled with the number of contact events and/or the CNT-microorganism contact area would also be anticipated should membrane lipid disruption or protein binding contribute to cell death.[50,80] Similarly, the magnitude of oxidative stress generated by CNTs would also increase with CNT loading.[43,50−52]

In terms of broader environmental implications, this investigation reveals that the cytotoxicity of CNTs will be preserved for both SWNCTs and MWCNTs embedded in commercial products after oxidation. Consistent with previous studies, our results demonstrate the necessity for direct contact to exist between surface-bound CNTs and attached microorganisms for antimicrobial effects to occur, with the caveat that not every CNT-microorganism interaction leads to cell death.[43,44,47,59,60,77] In most commercial products where CNTs are not directly exposed to the surrounding environment, antimicrobial properties will not manifest themselves until CNTs are exposed at the surface of the material (e.g., after a coating has been degraded). However, even under these conditions, CNT-containing surfaces cannot be considered truly antimicrobial since the onset of biofilm growth will only be slowed by the presence of surface-bound CNTs but not inhibited.

■ ASSOCIATED CONTENT

Supporting Information

Additional information on spray-coating (Figure S1); SEM analysis; CNT broadening in SEM; replicate images at each nanocomposite loading (Figure S2); details of XPS analysis and spectra of O-SWCNT/PVOH nanocomposites (Figure S3); qualitative SEM dissolution controls (Figures S4 and S5); replicate CLSM images of LIVE/DEAD stained *P. aeruginosa* on PVOH, 10% w/w O-MWCNT/PVOH, and 10% w/w O-SWCNT/PVOH nanocomposites from three separately grown cultures to showcase cell attachment consistency in the CLSM data (Figure S6); microbial frozen stock preparation; growth curves in LB broth with kinetic analysis (Figure S7); BMM media composition, microbial growth procedures; growth curves in BMM with and without 90 ppb O-SWCNTs and O-MWCNTs with kinetic analysis (Figure S8); details of the LIVE/DEAD staining procedure, a CLSM image of LIVE/DEAD stained *P. aeruginosa* grown on PVOH for 6 h (Figure S9); a CLSM image of a dead control where *P. aeruginosa* was intentionally lysed with ethanol and LIVE/DEAD stained (Figure S10); details of CLSM; details of the LIVE/DEAD cell counting software analysis; LIVE/DEAD stained background fluorescence controls (Figure S11); cell attachment controls (Figure S12); fluorescence photobleaching and quenching controls (Figures S13 and S14); EPS staining and EPS stain background fluorescence controls (Figures S16 and 17); spatial comparison of *P. aeruginosa* on 1% w/w O-MWCNT and O-SWCNT/PVOH nanocomposites using SEM with "live-on-dead" structures shown in CLSM (Figures S18 and S19), SEM microbial fixation procedure details and images of *P. aeruginosa* on PVOH and 10% w/w O-MWCNT/PVOH (Figure S20); antimicrobial trends on O-MWCNT/PVOH and O-SWCNT/PVOH nanocomposites as a function of surface CNT loading (Figure S21); an illustration of the number density effect of O-MWCNTs versus O-SWCNTs in PVOH at 1% w/w with respect to microorganism attachment (Figure S22); ICP-MS analysis of metal ion release (Figure S23); sp-ICP-MS analysis of CNT release using ^{89}Y as a proxy for CNTs released from nanocomposites in this study; a CLSM image of LIVE/DEAD stained *P. aeruginosa* on hydrophobic PCL (Figure S24); and a table of CNT metal content as determined by energy dispersive X-ray analysis (EDS). This material is available free of charge via the Internet at http://pubs.acs.org.

■ AUTHOR INFORMATION

Corresponding Author

*Phone: 410-516-4328. E-mail: howardf@jhu.edu.

Notes

Disclosure: Certain commercial entities, equipment, or materials may be identified in this document in order to describe an experimental procedure or concept adequately. Such identification is not intended to imply recommendation or endorsement by the National Institute of Standards and Technology, nor is it intended to imply that the entities, materials, or equipment are necessarily the best available for the purpose.

The authors declare no competing financial interest.

■ ACKNOWLEDGMENTS

The authors would like to thank Marielle Remillard, Julie Bitter, and Miranda Gallagher for their contributions as well as Dr. Michael McCaffery, Alice Sanchez, and Erin Pryce of the Integrated Imaging Center for their guidance in image acquisition, processing, and development of image analysis software. Additionally, we would like to acknowledge Mark Koontz for his help in acquiring the SEM images and Jingjing Wang and Jim Ranville from the Colorado School of Mines for their analysis of metal ion release. The authors would also like to thank the JHU INBT Pilot Project, the NSF (CBET #1236493), and the Owens Graduate Fellowship for their financial support.

■ REFERENCES

(1) McClory, C.; Chin, S. J.; McNally, T. Polymer/Carbon Nanotube Composites. *Aust. J. Chem.* **2009**, *62* (8), 762−785.

(2) Jones, W. E., Jr.; Chiguma, J.; Johnson, E.; Pachamuthu, A.; Santos, D. Electrically and thermally conducting nanocomposites for electronic applications. *Materials* **2010**, *3* (2), 1478−1496.

(3) Esawi, A. M. K.; Farag, M. M. Carbon nanotube reinforced composites: Potential and current challenges. *Mater. Des.* **2007**, *28*, 2394−2401.

(4) Rahmat, M.; Hubert, P. Carbon nanotube-polymer interactions in nanocomposites: A review. *Compos. Sci. Technol.* **2011**, *72* (1), 72−84.

(5) Gangopadhyay, R.; De, A. Conducting Polymer Nanocomposites: A Brief Overview. *Chem. Mater.* **2000**, *12* (3), 608−622.

(6) Moniruzzaman, M.; Winey, K. I. Polymer nanocomposites containing carbon nanotubes. *Macromolecules* **2006**, *39* (16), 5194−5205.

(7) Sahoo, N. G.; Rana, S.; Cho, J. W.; Li, L.; Chan, S. H. Polymer nanocomposites based on functionalized carbon nanotubes. *Prog. Polym. Sci.* **2010**, *35* (7), 837−867.

(8) Du, J.; Bai, J.; Cheng, H. The present status and key problems of carbon nanotube based polymer composites. *eXPRESS Polym. Lett.* **2007**, *1* (5), 253−273.

DOI: 10.1021/acs.est.5b00084
Environ. Sci. Technol. 2015, 49, 5484−5492

(9) Allaoui, A.; Bai, S.; Cheng, H. M.; Bai, J. B. Mechanical and electrical properties of a MWNT/epoxy composite. *Compos. Sci. Technol.* **2002**, *62* (15), 1993−1998.
(10) Ajayan, P. M.; Schadler, L. S.; Giannaris, C.; Rubio, A. Single-walled carbon nanotube-polymer composites: strength and weakness. *Adv. Mater. (Weinheim, Ger.)* **2000**, *12* (10), 750−753.
(11) Baughman, R. H.; Zakhidov, A. A.; de Heer, W. A. Carbon nanotubes - the route toward applications. *Science* **2002**, *297* (5582), 787−792.
(12) Coleman, J. N.; Khan, U.; Blau, W. J.; Gun'ko, Y. K. Small but strong: A review of the mechanical properties of carbon nanotube-polymer composites. *Carbon* **2006**, *44* (9), 1624−1652.
(13) Lau, K. T. Interfacial bonding characteristics of nanotube/polymer composites. *Chem. Phys. Lett.* **2003**, *370* (3−4), 399−405.
(14) Lau, K. T.; Hui, D. Effectiveness of using carbon nanotubes as nano-reinforcements for advanced composite structures. *Carbon* **2002**, *40* (9), 1605−1606.
(15) Rahmat, M.; Das, K.; Hubert, P. Interaction stresses in carbon nanotube-polymer nanocomposites. *ACS Appl. Mater. Interfaces* **2011**, *3* (9), 3425−3431.
(16) Qian, D.; Dickey, E. C.; Andrews, R.; Rantell, T. Load transfer and deformation mechanisms in carbon nanotube-polystyrene composites. *Appl. Phys. Lett.* **2000**, *76* (20), 2868−2870.
(17) Mylvaganam, K.; Zhang, L. C. Fabrication and application of polymer composites comprising carbon nanotubes. *Recent Pat. Nanotechnol.* **2007**, *1* (1), 59−65.
(18) Martin, C. A.; Sandler, J. K. W.; Shaffer, M. S. P.; Schwarz, M. K.; Bauhofer, W.; Schulte, K.; Windle, A. H. Formation of percolating networks in multi-wall carbon-nanotube-epoxy composites. *Compos. Sci. Technol.* **2004**, *64* (15), 2309−2316.
(19) Sandler, J. K. W.; Kirk, J. E.; Kinloch, I. A.; Shaffer, M. S. P.; Windle, A. H. Ultra-low electrical percolation threshold in carbon-nanotube-epoxy composites. *Polymer* **2003**, *44* (19), 5893−5899.
(20) Lu, D. D.; Li, Y. G.; Wong, C. P. Recent advances in nano-conductive adhesives. *J. Adhes. Sci. Technol.* **2008**, *22* (8−9), 815−834.
(21) Li, J.; Lumpp, J. K.; Andrews, R.; Jacques, D. Aspect ratio and loading effects of multiwall carbon nanotubes in epoxy for electrically conductive adhesives. *J. Adhes. Sci. Technol.* **2008**, *22* (14), 1659−1671.
(22) Paik, K. W.; Han, S. H. A study on B-stage CNT/epoxy composite films for electronic packaging applications. *Mater. Sci. Forum* **2010**, *654−656*, 2755−2758 PRICM 7, Pts 1−3.
(23) (WWICS) Woodrow Wilson International Center for Scholars "The Project on Emerging Nanotechnologies" Nanotechnology Consumer Products Inventory. http://www.nanotechproject.org/inventories/consumer/ (accessed Mar 31, 2015).
(24) Duncan, T. V. Applications of nanotechnology in food packaging and food safety: Barrier materials, antimicrobials and sensors. *J. Colloid Interface Sci.* **2011**, *363* (1), 1−24.
(25) Nanocyl carbon nanotube applications: fuel system components. http://www.nanocyl.com/Products-Solutions/Sectors/Automotive/Fuel-System-Components(accessed Mar 31, 2015).
(26) Soulestin, J.; Prashantha, K.; Lacrampe, M. F.; Krawczak, P. *Bioplastics based nanocomposites for packaging applications*; 2011.
(27) De, V. M. F. L.; Tawfick, S. H.; Baughman, R. H.; Hart, A. J. Carbon nanotubes: Present and future commercial applications. *Science (Washington, DC, U. S.)* **2013**, *339* (6119), 535−539.
(28) Petersen, E. J.; Zhang, L. W.; Mattison, N. T.; O'Carroll, D. M.; Whelton, A. J.; Uddin, N.; Nguyen, T.; Huang, Q. G.; Henry, T. B.; Holbrook, R. D.; Chen, K. L. Potential release pathways, environmental fate, and ecological risks of carbon nanotubes. *Environ. Sci. Technol.* **2011**, *45* (23), 9837−9856.
(29) Hirth, S.; Cena, L.; Cox, G.; Tomović, Ž.; Peters, T.; Wohlleben, W. Scenarios and methods that induce protruding or released CNTs after degradation of nanocomposite materials. *J. Nanopart. Res.* **2013**, *15* (4), 1−15.
(30) Kingston, C.; Zepp, R.; Andrady, A.; Boverhof, D.; Fehir, R.; Hawkins, D.; Roberts, J.; Sayre, P.; Shelton, B.; Sultan, Y.; Vejins, V.; Wohlleben, W. Release characteristics of selected carbon nanotube polymer composites. *Carbon* **2014**, *68* (0), 33−57.
(31) Gottschalk, F.; Nowack, B. The release of engineered nanomaterials to the environment. *J. Environ. Monit.* **2011**, *13* (5), 1145−1155.
(32) Ging, J.; Tejerina-Anton, R.; Ramakrishnan, G.; Nielsen, M.; Murphy, K.; Gorham, J. M.; Nguyen, T.; Orlov, A. Development of a conceptual framework for evaluation of nanomaterials release from nanocomposites: Environmental and toxicological implications. *Sci. Total Environ.* **2014**, *473*, 9−19.
(33) Nguyen, T.; Pelligrin, B.; Bernard, C.; Gu, X.; Gorham, J. M.; Stutzman, P.; Stanley, D.; Shapiro, D.; Bryrd, E.; Hettenhouse, R.; Chin, J. Fate of nanoparticles during life cycle of polymer nanocomposites. *J. Phys.: Conf. Ser.* **2011**, *34*, 012060.
(34) Costerton, J. W.; Cheng, K. J.; Geesey, G. G.; Ladd, T. I.; Nickel, J. C.; Dasgupta, M.; Marrie, T. J. Bacterial biofilms in Nature and disease. *Annu. Rev. Microbiol.* **1987**, *41*, 435−64.
(35) Andersson, S.; Rajarao, G. K.; Land, C. J.; Dalhammar, G. Biofilm formation and interactions of bacterial strains found in wastewater treatment systems. *FEMS Microbiol. Lett.* **2008**, *283* (1), 83−90.
(36) Francolini, I.; Norris, P.; Piozzi, A.; Donelli, G.; Stoodley, P. Usnic acid, a natural antimicrobial agent able to inhibit bacterial biofilm formation on polymer surfaces. *Antimicrob. Agents Chemother.* **2004**, *48* (11), 4360−4365.
(37) Carlson, R. P.; Taffs, R.; Davison, W. M.; Stewart, P. S. Anti-biofilm properties of chitosan-coated surfaces. *J. Biomater. Sci., Polym. Ed.* **2008**, *19* (8), 1035−1046.
(38) Leja, K.; Lewandowicz, G. Polymer Biodegradation and Biodegradable Polymers−A Review. *Pol. J. Environ. Stud.* **2010**, *13* (2), 255−266.
(39) Shah, A. A.; Hasan, F.; Hameed, A.; Ahmed, S. Biological degradation of plastics: A comprehensive review. *Biotechnol. Adv.* **2008**, *26* (3), 246−265.
(40) Sivan, A. New Perspectives in Plastic Biodegradation. *Curr. Opin. Biotechnol.* **2011**, *22* (3), 422−426.
(41) Tokiwa, Y.; Calabia, B. P.; Ugwu, C. U.; Alba, S. Biodegradability of Plastics. *Int. J. Mol. Sci.* **2009**, *10* (9), 3722−3742.
(42) Rodrigues, D. F.; Elimelech, M. Toxic effects of single-walled carbon nanotubes in the development of *E. coli* biofilm. *Environ. Sci. Technol.* **2010**, *44* (12), 4583−4589.
(43) Kang, S.; Herzberg, M.; Rodrigues, D. F.; Elimelech, M. Antibacterial effects of carbon nanotubes: Size does matter. *Langmuir* **2008**, *24* (13), 6409−6413.
(44) Kang, S.; Pinault, M.; Pfefferle, L. D.; Elimelech, M. Single-walled carbon nanotubes exhibit strong antimicrobial activity. *Langmuir* **2007**, *23* (17), 8670−8673.
(45) Liu, S.; Wei, L.; Hao, L.; Fang, N.; Chang, M. W.; Xu, R.; Yang, Y.; Chen, Y. Sharper and faster "nano darts" kill more bacteria: a study of antibacterial activity of individually dispersed pristine single-walled carbon nanotube. *ACS Nano* **2009**, *3* (12), 3891−3902.
(46) Alpatova, A. L.; Shan, W. Q.; Babica, P.; Upham, B. L.; Rogensues, A. R.; Masten, S. J.; Drown, E.; Mohanty, A. K.; Alocilja, E. C.; Tarabara, V. V. Single-walled carbon nanotubes dispersed in aqueous media via non-covalent functionalization: Effect of dispersant on the stability, cytotoxicity, and epigenetic toxicity of nanotube suspensions. *Water Res.* **2010**, *44* (2), 505−520.
(47) Ahmed, F.; Santos, C. M.; Vergara, R. A. M. V.; Tria, M. C. R.; Advincula, R.; Rodrigues, D. F. Antimicrobial applications of electroactive PVK-SWNT nanocomposites. *Environ. Sci. Technol.* **2012**, *46* (3), 1804−1810.
(48) Arias, L. R.; Yang, L. Inactivation of Bacterial Pathogens by Carbon Nanotubes in Suspensions. *Langmuir* **2009**, *25* (5), 3003−3012.
(49) Aslan, S.; Loebick, C. Z.; Kang, S.; Elimelech, M.; Pfefferle, L. D.; Van, T. P. R. Antimicrobial biomaterials based on carbon nanotubes dispersed in poly(lactic-co-glycolic acid). *Nanoscale* **2010**, *2* (9), 1789−1794.
(50) Vecitis, C. D.; Zodrow, K. R.; Kang, S.; Elimelech, M. Electronic-Structure-Dependent Bacterial Cytotoxicity of Single-Walled Carbon Nanotubes. *ACS Nano* **2010**, *4* (9), 5471−5479.

DOI: 10.1021/acs.est.5b00084
Environ. Sci. Technol. 2015, 49, 5484−5492

(51) Pasquini, L. M.; Hashmi, S. M.; Sommer, T. J.; Elimelech, M.; Zimmerman, J. B. Impact of surface functionalization on bacterial cytotoxicity of single-walled carbon nanotubes. *Environ. Sci. Technol.* **2012**, *46* (11), 6297−6305.
(52) Pasquini, L. M.; Sekol, R. C.; Taylor, A. D.; Pfefferle, L. D.; Zimmerman, J. B. Realizing Comparable Oxidative and Cytotoxic Potential of Single- and Multiwalled Carbon Nanotubes through Annealing. *Environ. Sci. Technol.* **2013**, *47* (15), 8775−8783.
(53) Yang, C.; Mamouni, J.; Tang, Y.; Yang, L. Antimicrobial Activity of Single-Walled Carbon Nanotubes: Length Effect. *Langmuir* **2010**, *26* (20), 16013−16019.
(54) Qi, X.; Poernomo, G.; Wang, K.; Chen, Y.; Chan-Park, M. B.; Xu, R.; Chang, M. W. Covalent immobilization of nisin on multi-walled carbon nanotubes: superior antimicrobial and anti-biofilm properties. *Nanoscale* **2011**, *3* (4), 1874−1880.
(55) Woerle-Knirsch, J. M.; Pulskamp, K.; Krug, H. F. Oops they did it again! Carbon nanotubes hoax scientists in viability assays. *Nano Lett.* **2006**, *6* (6), 1261−1268.
(56) Pantanella, F.; Berlutti, F.; Passeri, D.; Sordi, D.; Frioni, A.; Natalizi, T.; Terranova, M. L.; Rossi, M.; Valenti, P. Quantitative evaluation of bacteria adherent and in biofilm on single-wall carbon nanotube-coated surfaces. *Interdiscip. Perspect. Infect. Dis.* **2011**, *2011*, 1−9.
(57) Hussain, M.; Kabir, M.; Sood, A. On the cytotoxicity of carbon nanotubes. *Curr. Sci.* **2009**, *96* (5), 664−673.
(58) Du, J.; Wang, S.; You, H.; Zhao, X. Understanding the toxicity of carbon nanotubes in the environment is crucial to the control of nanomaterials in producing and processing and the assessment of health risk for human: A review. *Environ. Toxicol. Pharmacol.* **2013**, *36* (2), 451−462.
(59) Santos, C. M.; Milagros Cui, K.; Ahmed, F.; Tria, M. C. R.; Vergara, R. A. M. V.; de Leon, A. C.; Advincula, R. C.; Rodrigues, D. F. Bactericidal and anticorrosion properties in PVK/MWNT nanocomposite coatings on stainless steel. *Macromol. Mater. Eng.* **2012**, *297* (8), 807−813.
(60) Schiffman, J. D.; Elimelech, M. Antibacterial activity of electrospun polymer mats with incorporated narrow diameter single-walled carbon nanotubes. *ACS Appl. Mater. Interfaces* **2011**, *3* (2), 462−468.
(61) Mauter, M. S.; Elimelech, M. Environmental applications of carbon-based nanomaterials. *Environ. Sci. Technol.* **2008**, *42* (16), 5843−5859.
(62) Upadhyayula, V. K. K.; Gadhamshetty, V. Appreciating the role of carbon nanotube composites in preventing biofouling and promoting biofilms on material surfaces in environmental engineering: a review. *Biotechnol. Adv.* **2010**, *28* (6), 802−816.
(63) Jones, P. H.; Prasad, D.; Heskins, M.; Morgan, M. H.; Guillet, J. E. Biodegradability of photodegraded polymers. I. Development of experimental procedures. *Environ. Sci. Technol.* **1974**, *8* (10), 919−923.
(64) Guillet, J. E.; Regulski, T. W.; McAneney, T. B. Biodegradability of photodegraded polymers. II. Tracer studies of biooxidation of Ecolyte PS polystyrene. *Environ. Sci. Technol.* **1974**, *8* (10), 923−925.
(65) Nguyen, T.; Pellegrin, B.; Mermet, L.; Shapiro, A.; Gu, X.; Chin, J. Network aggregation of CNTs at the surface of epoxy/MWCNT composite exposed to UV radiation. *Nanotechnology* **2009**, 90−3.
(66) Hou, W.-C.; BeigzadehMilani, S.; Jafvert, C. T.; Zepp, R. G. Photoreactivity of unfunctionalized single-wall carbon nanotubes involving hydroxyl radical: Chiral dependency and surface coating effect. *Environ. Sci. Technol.* **2014**, *48* (7), 3875−3882.
(67) Qu, X.; Alvarez, P. J.; Li, Q. Photochemical transformation of carboxylated multiwalled carbon nanotubes: Role of reactive oxygen species. *Environ. Sci. Technol.* **2013**, *47* (24), 14080−14088.
(68) Chiellini, E.; Corti, A.; Solaro, R. Biodegradation of poly(vinyl alcohol) based blown films under different environmental conditions. *Polym. Degrad. Stab.* **1999**, *64* (2), 305−312.
(69) Tang, X.; Alavi, S. Recent advances in starch, polyvinyl alcohol based polymer blends, nanocomposites and their biodegradability. *Carbohydr. Polym.* **2011**, *85*, 7−18.
(70) Madigan, M. T.; Martinko, J. M.; Dunlap, P. V.; Clark, D. P. *Brock Biology of Microorganisms*, 12th ed.; Pearson: San Francisco, CA, 2009.
(71) Vickerman, J. C.; Gilmore, I. S. *Surface analysis: the principal techniques*; Wiley Online Library: 2009; Vol. 2.
(72) Tanuma, S.; Powell, C. J.; Penn, D. R. Calculations of electron inelastic mean free paths. II. Data for 27 elements over the 50−2000 eV range. *Surf. Interface Anal.* **1991**, *17* (13), 911−926.
(73) Reed, R. B.; Goodwin, D. G.; Marsh, K. L.; Capracotta, S. S.; Higgins, C. P.; Fairbrother, D. H.; Ranville, J. F. Detection of single walled carbon nanotubes by monitoring embedded metals. *Environ. Sci.: Processes Impacts* **2013**, *15* (1), 204−213.
(74) Invitrogen, FilmTracer LIVE/DEAD Biofilm Viability Kit. In Probes, M. Ed. 2009.
(75) Invitrogen, *FilmTracer SYPRO Ruby Biofilm Matrix Stain*. In Probes, M., Ed.; 2009.
(76) Petersen, E. J.; Lam, T.; Gorham, J. M.; Scott, K. C.; Long, C. J.; Stanley, D.; Sharma, R.; Alexander Liddle, J.; Pellegrin, B.; Nguyen, T. Methods to assess the impact of UV irradiation on the surface chemistry and structure of multiwall carbon nanotube epoxy nanocomposites. *Carbon* **2014**, *69*, 194−205.
(77) Kang, S.; Mauter, M. S.; Elimelech, M. Microbial Cytotoxicity of Carbon-Based Nanomaterials: Implications for River Water and Wastewater Effluent. *Environ. Sci. Technol.* **2009**, *43* (7), 2648−2653.
(78) Teitzel, G. M.; Parsek, M. R. Heavy metal resistance of biofilm and planktonic Pseudomonas aeruginosa. *Appl. Environ. Microbiol.* **2003**, *69* (4), 2313−2320.
(79) de Vicente, A.; Avilés, M.; Codina, J. C.; Borrego, J. J.; Romero, P. Resistance to antibiotics and heavy metals of Pseudomonas aeruginosa isolated from natural waters. *J. Appl. Bacteriol.* **1990**, *68* (6), 625−632.
(80) Corredor, C.; Hou, W.-C.; Klein, S. A.; Moghadam, B. Y.; Goryll, M.; Doudrick, K.; Westerhoff, P.; Posner, J. D. Disruption of model cell membranes by carbon nanotubes. *Carbon* **2013**, *60*, 67−75.

DOI: 10.1021/acs.est.5b00084
Environ. Sci. Technol. 2015, 49, 5484−5492